Inorganic Chemistry

Article

pubs.acs.org/IC

Pillared-Layer Cluster Organic Frameworks Constructed from Nanoscale Ln_{10} and Cu_{16} Clusters

Wei-Hui Fang and Guo-Yu Yang*

State Key Laboratory of Structural Chemistry, Fujian Institute of Research on the Structure of Matter, Chinese Academy of Sciences, 155 West Yangqiao Road, Fuzhou, Fujian 350002, China

Supporting Information

ABSTRACT: Two pillared-layer cluster organic frameworks, $[Ln_5(\mu_3\text{-}OH)_4(\mu\text{-}H_2O)Cu_8I_8L_{11}]\cdot H_2O$ (L = 4-pyridin-4-yl-benzoate; Ln = Dy(**1**), Eu(**2**)), have been made by employing lanthanide oxide and copper(I) halide as the source of lanthanide and transitional metal under hydrothermal condition. Compared to the pillared-layer frameworks constructed from heterometallic layers and organic pillars, these two compounds are derived from lanthanide cluster organic layers and copper(I) halide cluster motifs. Thus, there are two distinct types of inorganic metal connectors in the structure, one is hydroxo lanthanide $[Ln_{10}(\mu_3\text{-}OH)_8]^{22+}$ (Ln_{10}) cluster, and the other is copper(I) halide $[Cu_{16}I_{16}]$ (Cu_{16}) cluster. The rational assembly of these two inorganic connectors and organic linear linkers leads to the formation of the two complexes here. To the best of our knowledge, they appear to be the first 3D frameworks constructed from decanuclear hydroxo lanthanide clusters. From the topological point of view, these compounds represent an intriguing example of a binodal (8,14)-connected net considering the Ln_{10} and Cu_{16} connectors as the nodes, revealing that they are typical high dimensional frameworks with high connected net based on high nuclearity nodes. Furthermore, elemental analysis, IR, TGA, PXRD, and UV−vis properties are also studied.

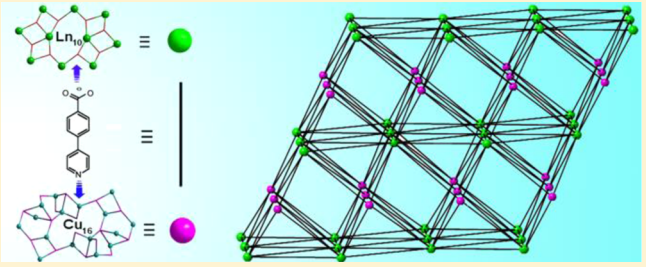

INTRODUCTION

Apart from the aesthetic perspective, the interest in nanoscale metal clusters arises from their novel properties and potential applications.[1] Although the cluster chemistry of transition metals (TMs) is now well-established,[2] the analogous chemistry of lanthanides (Ln) is less developed attributing to its variable and high coordination numbers as well as poor stereochemical preferences.[3] In general, the polynuclear hydroxo Ln clusters are assembled in combinations of one or two types of low nuclearity Ln cores.[4] For instance, the Dy_6 cluster is made up of two head-to-head triangles,[4a] and the Ln_{14} core is constructed from one octahedron and two corner-sharing square pyramids.[4d] So far, the largest TM core is Mo_{368},[2a] the largest Ln cluster is an Er_{60} cage featuring 24 vertex-sharing cubanes,[4e] and the largest heterometallic 3d−4f core is nanoscale $Cu^{II}_{36}Ln^{III}_{24}$[5a] metallo-rings. With respect to the heterometallic cluster organic compounds, most are discrete structures based on one type of mixed core;[5] extended frameworks constructed from distinct Ln and TM cores are rarely reported. Typical examples are sandwich frameworks constructed from two distinct layered networks of nanosized Ln^{III} and Cu^{I} wheels:[6] Ln_{18} and Cu_{24} in **FJ-4**, La_{18} and $3Cu@Cu_{24}$ in **FJ-21**, Ln_{24} and $Cu_2@Cu_{24}$ in **FJ-22**. Thus, the assembly of extended structures incorporating both Ln and TM clusters within the same crystal structure is still a challenge.

To construct extended heterometallic frameworks with both Ln and TMs clusters, a connector and linker approach is universally adopted. Obviously, Ln and TM clusters serve as connectors, and linkers refer to multidentate ligands that can simultaneously capture both Ln and TM connectors to form structures ranging from chains, to layers, to diversity nets (Scheme 1). So the primary issue is to obtain distinct connectors of high nuclearity Ln and TM cores. In fact, oxygen atoms prefer to bridge Ln ions, and inorganic halogen

Scheme 1. Scheme Representation of the Connector and Linker Approach

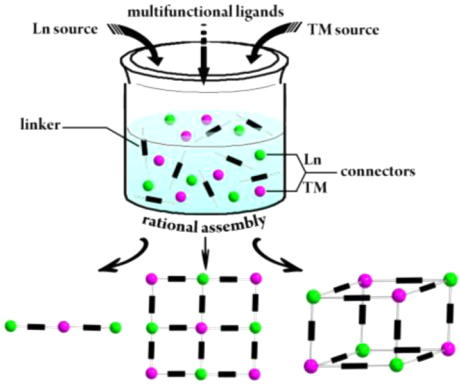

Received: February 19, 2014
Published: May 14, 2014

   dx.doi.org/10.1021/ic500404z | Inorg. Chem. 2014, 53, 5631−5636

atoms possess high affinities for monovalent copper ions. On the basis of the above considerations, we choose Ln oxide and copper(I) halide as the source of Ln and TM to obtain two types of distinct hydroxo Ln clusters and copper(I) halide clusters rather than one kind of mixed Ln−TM connectors. Another important issue is the judicious choice of linkers. To date, amino acids,[5b] betains,[7] and pyridinecarboxylate ligands[3,8] with mixed N/O donors have been proven to be effective linkers. Our group selected a multifunctional linear ligand, isonicotinic acid (HIN), with mixed N/O donors on opposite sides to join two types of connectors.

As expected, a series of 3D heterometallic frameworks based on distinct metal cores were obtained.[3,6a,8a] To maintain continuity with our previous study, lengthened HIN, 4-pyridin-4-yl-benzoic acid (HL),[9] is employed, with the expectation that this lengthened ligand is capable of linking distinct connectors of both Ln and Cu metal cores. Here, we describe the synthesis and characterization of $[Ln_5(\mu_3\text{-}OH)_4(\mu\text{-}H_2O)Cu_8I_8L_{11}]\cdot H_2O$ (Ln = Dy **1**, Eu **2**). Despite the decanuclear cluster Y_{10}[10] first described 20 years ago, less attention has paid to the syntheses of the decanuclear Ln cluster. Until now, there have been few known decanuclear clusters in combinatorial configurations reported yet (Figure 1a−c).[4b,11] Unfortunately, extended

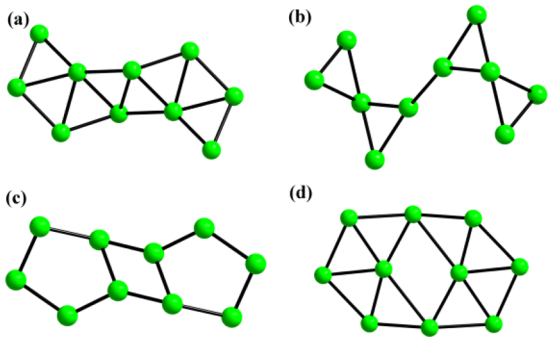

Figure 1. Arrangement of the reported decanuclear Ln cores in ref 4b (a), ref 11 (b,c), and this text (d).

frameworks based on decanuclear Ln cluster are scarcely reported,[12] and there are no three-dimensional (3D) frameworks have been document-ed up to date. Notably, compounds **1**−**2** represent the first 3D frameworks constructed from decanuclear hydroxo Ln clusters. Moreover, nanoscale Ln_{10} (Figure 1d) and Cu_{16} cores are simultaneously included.

EXPERIMENTAL SECTION

Materials and Physical Measurements. All chemicals and solvents were commercially purchased and used without further purification. The elemental analyses for C, H, and N were carried out using the combustion method on an Elemental Vario EL III CHNOS elemental analyzer. IR spectra (KBr pellets) were recorded on an ABB Bomem MB102 spectrometer over a range 400−4000 cm^{-1}. The thermogravimetric analyses were performed on a Mettler Toledo TGA/SDTA 851e analyzer in air atmosphere with a heating rate of 10 °C/min from 30 to 1000 °C. Powder X-ray diffraction (PXRD) data were collected on a Rigaku MiniFlex II diffractometer using Cu Kα radiation (λ = 1.540 56 Å) under ambient conditions. The UV−vis spectra were recorded at room temperature on a PE Lambda 950 UV−vis spectrometer.

Syntheses of 1−2. A mixture of Ln_2O_3 (0.4 mmol: Dy_2O_3 0.149 g; Eu_2O_3 0.141 g), CuI (0.8 mmol, 0.152 g), HL (2 mmol, 0.398 g), H_2O (10.0 mL, 0.22 mmol), and 0.5 M H_2SO_4 with the pH value of about 2.0 was sealed in a 30 mL Teflon-lined bomb at 200 °C for 7 days, and then cooled to room temperature. Dark red parallelepiped-shape crystals of **1**−**2** were recovered by filtration, washed with distilled water, and dried at ambient temperature (yield 45%, 36% based on Dy_2O_3 and Eu_2O_3). Anal. Calcd (%) for $C_{132}H_{96}Cu_8Dy_5I_8N_{11}O_{28}$ (**1**): C 34.31, H 2.09, N 3.33. Found: C 34.60, H 2.51, N 3.67. IR (cm^{-1}) for **1**: 3448 (m), 2361(w), 1642(m), 1603(s), 1550(vs), 1420(vs), 1223 (w), 1068(w), 829(w), 781(m), 663(w), 550(w). Anal. Calcd for $C_{132}H_{96}Cu_8Eu_5I_8N_{11}O_{28}$ (**2**): C 34.71, H 2.11, N 3.37. Found: C 35.04, H 2.48, N 3.74. IR (cm^{-1}) for **2**: 3447(m), 2360(w), 1641(m), 1602(s), 1551(vs), 1422(vs), 1222(w), 1190(w), 1062(w), 827(w), 780(m), 664(w), 549(w).

X-ray Crystallographic Analyses. The intensity data was collected on SATURN70 CCD diffractometer with graphite-monochromatized Mo Kα (λ = 0.710 73 Å) radiation at room temperature. All absorption corrections were performed using the multiscan program. The structures were solved by direct methods and refined by full-matrix least-squares on F^2 with the SHELXTL-97 program.[13] Non-hydrogen atoms were refined anisotropically. Selected crystallographic data and refinement details for **1** and **2** are summarized in Supporting Information Table S1, and selected bond lengths are listed in Supporting Information Table S2. CCDC numbers 951613 and 951614 contain the supplementary crystallographic data.

RESULTS AND DISCUSSION

Syntheses. In the past few decades, 3d−4f heterometallic frameworks have become an important member in the family of metal organic frameworks.[14] However, the inevitable competition among negative supporting ligands and positive Ln and Cu ions may result in homometallic complexes rather than heterometallic compounds, indicating the challenge aspect. Besides the conventional solution reactions, a hydrothermal technique has proven to be another feasible synthetic method, especially when solubility is extremely small. More complicated metastable phases will exist in the hydrothermal system resulting from the high pressure and temperature. Considering the solubility of raw materials and environmental friendliness, a hydrothermal technique is employed. In this Article, we select Ln_2O_3 and CuI, including two different inorganic anions, as the source of Ln and TM to reduce the competition and generate two types of polynuclear clusters. Meanwhile, a multifunctional ligand with mixed N/O donors as linker to induce Ln and Cu ions undergoes its respective aggregations so as to construct two different connectors. Compounds **1**−**2** are successfully obtained by the hydrothermal treatment of Ln_2O_3 (Ln = Dy and Eu), CuI, and HL at 200 °C for 7 days in the presence of H_2SO_4 (pH = 2). Despite other lanthanide oxides being employed under the same conditions, unfortunately, only amorphous precipitates are observed instead. It seems that the size of the Ln ion can influence the crystallizing process.[15] In addition, H_2SO_4 is required to adjust the pH value during the assembly of these compounds, even though it does not exist in the final structures, for there are no crystals isolated when it is removed from the system. The composition of the products is confirmed by elemental analyses and IR spectra. The characteristic features of carboxyls dominate the IR spectra of **1**−**2** (Supporting Information Figure S1). The strong and acuity absorption bands around 3400 cm^{-1} are assigned as the characteristic peaks of −OH vibration. The strong vibrations from 1600 to 1400 cm^{-1} correspond to the asymmetric and symmetric stretching vibrations of the carboxyls. The collapse of strong bands around 1700 cm^{-1} indicates that the HL ligands are deprotonated. Furthermore, their phase purity was identified by PXRD patterns (Supporting Information Figure S2). The main peak positions presented in the experimental

dx.doi.org/10.1021/ic500404z | Inorg. Chem. 2014, 53, 5631−5636

patterns are coincident with those observed in the simulated patterns, revealing the phase purity of the samples. The differences in intensity may be attributed to the variation in preferred orientation of the powder sample during the collection of the experimental PXRD pattern.

Structure Description. Crystal structure analyses reveal that **1**−**2** are isostructural. As a representative, only the structure of **1** is described in detail. Compound **1** crystallizes in the monoclinic space group *C*2/*c*, and the asymmetric unit is composed of five crystallographically unique Dy^{3+} ions, eight Cu^{+} ions, eight I^{-} ions, four hydroxyl groups, one bridging and one lattice water molecules, as well as 11 L ligands with four types of coordination modes in the ratio 1:8:1:1 (Figure 2,

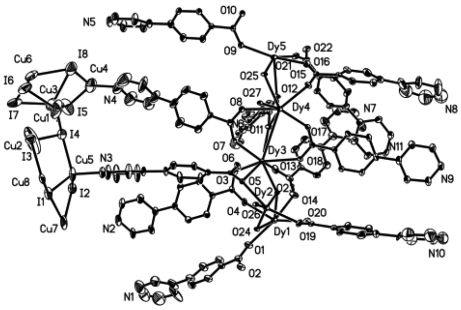

Figure 2. ORTEP drawing (30% probability level) of compound **1**. Lattice water molecules are omitted for clarity.

Scheme 2. Coordination Modes of the L Ligands in 1

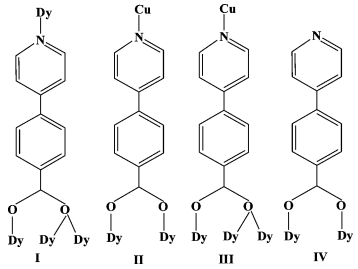

Scheme 2). The coordinate numbers of the five Dy ions rang from seven to nine: Dy1, Dy3 are in bicapped trigonal prism geometry; Dy2, Dy4, and Dy5 are in distorted monocapped, square antiprism and tricapped configurations, respectively (Supporting Information Figure S3). The Dy−O bond lengths range from 2.337(6) to 2.696(6) Å, with an average value of 2.485 Å, which is in accord with the related Dy compounds (Supporting Information Table S1).[3,6a] Eight Cu ions display two types of coordination modes: trigonal (Cu2, Cu3) and distorted tetrahedral (Cu1, Cu4, Cu5, Cu6, Cu7, Cu8) geometries.

There are two nanoscale crown-like clusters in **1**: decanuclear $[Dy_{10}(\mu_3\text{-OH})_8]^{22+}$ (Dy_{10}) and hexadecanuclear $[Cu_{16}I_{16}]$ (Cu_{16}) clusters (Figure 3). The Dy_{10} and Cu_{16} cores are almost coplanar with an average deviation from their respective plane of 0.32 and 0.89 Å. The first connector of Dy_{10} can be intuitively regarded as a slightly slipped sandwich configuration. Each half of the sandwich contains a roughly planar set of five Dy^{3+} ions in a trapezoid arrangement, which can be viewed as three edge-sharing triangles with each bearing a capped μ_3-OH group. The Dy_{10} core has an external diameter of 1.2 nm and an

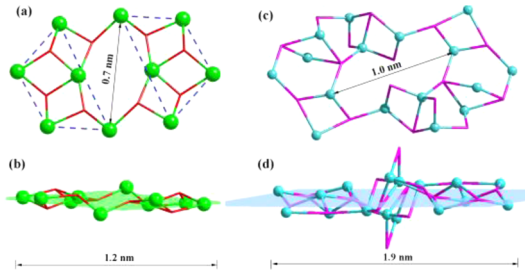

Figure 3. Top and side view of the Dy_{10} cluster (a,b) and the Cu_{16} cluster (c,d). Color codes: green Dy; blue Cu; red O; pink I.

inner olive-shaped 4-ring with a diameter of 0.7 nm (Figure 3a,b). With respect to the reported Tb_{10},[4b] the stagger angle (43.4°) and slide distance (5.4 Å) of two trapezoids are much larger than those (18.2° and 1.2 Å) here (Figure 4). As a result,

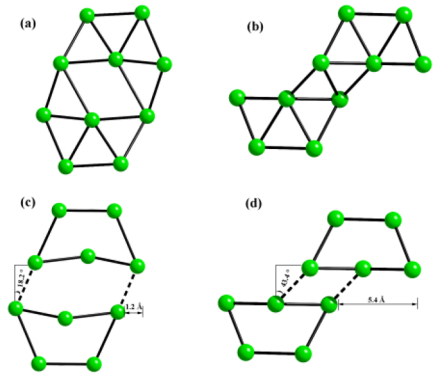

Figure 4. (a,b) Metal skeletons of the Dy_{10} cluster in **1** and the Tb_{10} cluster in ref 4b. (c,d) Schematic representation of the arrangements of the two trapezoid subunits.

an "open" Tb_{10} in "S" configuration is obtained, and a "closed" Dy_{10} with eight edge-sharing defected cubane units are observed in **1**. Peripheral coordination environment of the Dy_{10} connector is provided by two water bridges and 26 deprotonated L ligands with four coordination modes in the ratio 2:8:1:2 (Figure 5). Generally speaking, the Ln ions prefer

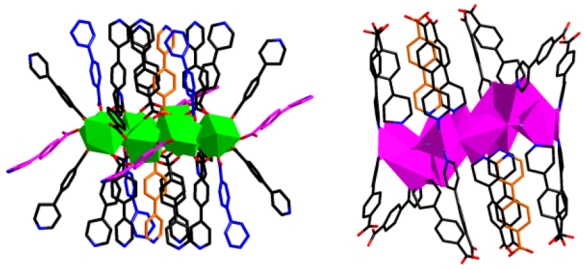

Figure 5. Coordination environments of the Ln_{10} (left) and Cu_{16} (right) clusters. The L ligands in modes I−IV are represented in pink, black, orange, and blue, respectively.

O to N donors, and the d-block TM ions have a much stronger tendency to coordinate to N donors. However, to our surprise, the pyridine nitrogen atom (N_{PY}) of L ligand in mode I directly bonds to the Dy^{3+} ion rather than the Cu^{+} ion as unambiguously revealed by single-crystal X-ray diffraction. Such a phenomenon can rarely be observed in a minority of Ln coordination polymers.[16] As shown in Figure 6a, the Dy_{10}

dx.doi.org/10.1021/ic500404z | Inorg. Chem. 2014, 53, 5631−5636

cores are bridged by water molecules to be a ribbon-like chain along the [010] direction.

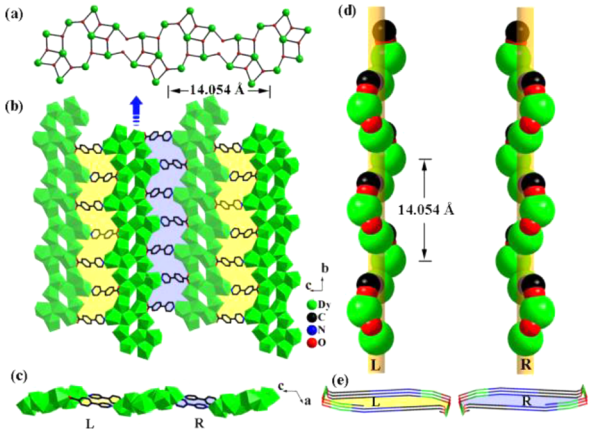

Figure 6. (a) One-dimensional Ln chain constructed from Dy_{10} units along the *b* axis. (b,c) Top and side view of the 2D Ln−organic layer. (d,e) Space-filling and wire view of the helical arrays.

Different from the organic linkers of the Ln cluster organic chains,[17] the linkers in the Dy_{10}-cluster-based chain are inorganic water ligands (Figure 6a). In addition, it is further confirmed that, except inorganic polyoxometalates[18] and germanate[19] chains being made in our laboratory, inorganic Ln cluster chains[20] can also be made though Ln ions have variable and high coordination numbers. Here, adjacent inorganic chains with reverse orientation in **1** are extended via L ligands in mode I generating Ln cluster organic layer on the *bc* plane (Figure 6b,c). Obviously, the L ligands in mode I play an important role in the formation of the Ln cluster organic layer. Actually, the Dy_{10} clusters are quite far from each other: the distance between neighboring clusters within the same inorganic chain is 14.054 Å, and the distance of two adjacent Dy_{10} clusters belonging to adjacent chains is 21.661 Å. Consequently, such Ln−organic layer can be viewed as a 6-connected *hxl* net considering the Dy_{10} clusters as the nodes (Figure 7). It is worth noting that the reverse orientation of the inorganic chains creates narrow and long curvatures that lead to the formation of helical arrays. There are a pair of helical channels along the [010] direction (Figure 6d,e). The helices contain left-helical chains and right-helical chains with a pitch of 14.054 Å (equivalent to the length of the *b* axis) running along the 2_1 axis.

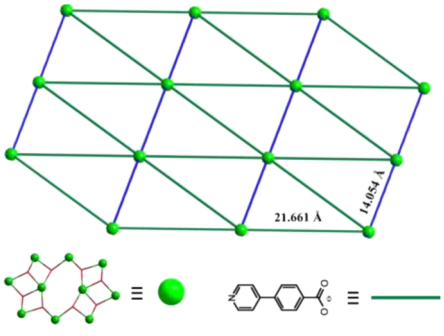

Figure 7. Topology of Ln−organic layer in compound **1**. The linkers of bridging water molecules and L ligands are represented in blue and green lines.

Despite diverse copper(I) halide cores ranging from rhomboid dimer to giant Cu_{36} being well-documented,[21] natural Cu_{16} core is rarely observed. The second connector here is Cu_{16} core with an external diameter of 1.9 nm and an inner peanut-like 6-ring with a diameter of 1.0 nm (Figure 3c,d). Peripheral coordination environment of the Cu_{16} core is completed by 18 deprotonated L ligands with modes II and III in the ratio 8:1 (Figure 5). Then, the Cu_{16} cores and the Ln cluster organic layers are pillared by the L ligands in modes II and III generating a fascinating 3D pillared-layer cluster organic framework (Figure 8a). To further stabilize the 3D framework,

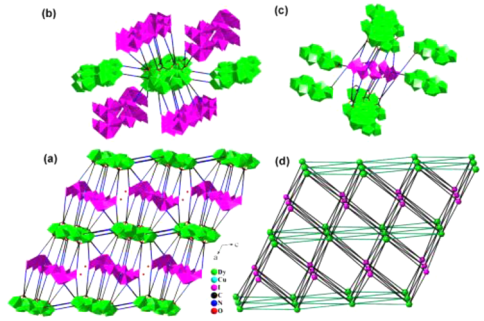

Figure 8. (a) Overall framework of **1** viewed along the *b* axis. The benzene and pyridine rings of L ligands are shown in lines for clarity. (b,c) The coordination environments of the Dy_{10} (green) and Cu_{16} (pink) cores. For clarification, blue lines represent benzene and pyridine rings of L linkers. (d) Schematic representation of the (8,14)-connected net. Dy_{10} and Cu_{16} clusters are represented as green and pink atoms; the *hxl* nets of Ln layers are emphasized in green lines.

the remaining L ligands in mode IV only serve as dangling arms using the carboxylate groups to bridge pairs of Dy^{3+} ions in the Dy_{10} cores, leaving the nitrogen atom uncoordinated. It is reported that the pore heights of pillared-layer structures can be altered by pillars, but their pore widths, determined by the layers, are almost unchangeable.[9a] Since the ligands are lengthened here, long and narrow porous are observed, where guest water molecules are located. Notably, pillared-layer frameworks ubiquitously exist in borates,[22] polyoxotungstates,[23] and TM[24] and Ln[25] compounds. Nevertheless, there are two types of heterometallic pillared-layer frameworks: one is constructed from heterometallic layers and organic pillars;[26] the other is based on pure Ln cluster organic layers and the pillars built by the Cu−halide cluster and the organic ligands (Scheme 3).[6,8a,9e,27] Compound **1** belongs to the latter one; the distance between the neighboring layers are obviously doubled. Notice that the Ln cluster units of the reported Ln organic layers are almost coplanar, displaying ribbon-like or wheel-shape, such as Ln_2,[27a] Ln_4,[9e] Ln_{16},[27b] Ln_{18},[6a] Ln_{24},[6b] and Er_{36},[8a] etc.

Scheme 3. Scheme Representation of the Two Types of Pillared-Layer Heterometallic Frameworks

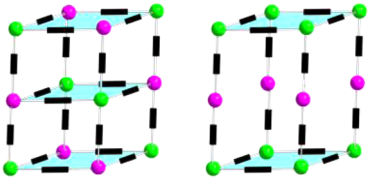

dx.doi.org/10.1021/ic500404z | Inorg. Chem. 2014, 53, 5631−5636

To better understand the complicated structure of **1**, the topological analysis approach is employed.[28] As shown in Figure 8b,c, every Dy_{10} connector is linked to six Dy_{10} neighbors and eight Cu_{16} cores through two water bridges and 26 linear linkers, while each Cu_{16} connector is surrounded by eight nearest Dy_{10} cores through 18 linear linkers. Therefore, the framework of **1** can be rationalized as a binodal (8,14)-connected net with Schläfli symbol of $(3^{10}.4^{14}.5^4)(3^{26}.4^{44}.5^{19}.6^2)$ by assigning Ln_{10} and Cu_{16} cores as nodes (Figure 8d). To date, there are relatively rare examples of high connected binodal networks.[29] One effective strategy for constructing such nets is to employ polynuclear units as connected nodes. The reported (8,14)-connected network here represents a good example of employing two types of polynuclear metal clusters to construct a highly connected binodal net. According to approach to the analysis of highly connected frameworks based on the visualization of the structures as combinations of interconnected layered 2D sheets or subnets,[30] the (8,14)-connected net can be described as the parallel 6-connected Ln layers (*hxl*) cross-linked by Cu_{16} cores in the two adjacent layers.

To study the thermal stabilities of **1**−**2**, TG analyses were carried out (Supporting Information Figure S4). They show similar thermal behavior and undergo two steps of weight loss. The water molecules and hydroxyls are gradually lost in the temperature range 30−300 °C. Above that temperature, the weight loss is due to the decomposition of the organic ligands and the collapse of the whole framework. Assuming that the residue corresponds to Ln_2O_3 and CuO, the observed weight is in good agreement with the calculated value (calcd/found **1** 34.0%/34.5%; **2** 33.3%/33.8%). Motivated by the presence of copper halide motifs revealed by single-crystal diffraction results, the optical diffuse reflectance spectra of **1**−**2** in the solid state were measured (Supporting Information Figure S5). Optical absorption spectra indicate that **1**−**2** exhibit strong and similar optical absorption with estimated optical band gaps of 2.16 and 2.18 eV, according to the Kubelka−Munk function.[31] These band gap sizes are significantly smaller than previous literature of CuI (2.92 eV).[6a]

CONCLUSIONS

In summary, we have successfully made and characterized two pillared-layer frameworks constructed from two distinct nanosized Dy_{10} and Cu_{16} connectors. To the best of our knowledge, they appear to be the first 3D frameworks derived from decanuclear hydroxo Ln clusters. Topology analyses indicate that they are unique binodal highly (8,14)-connected frameworks based on these two types of nanosized cores. It should be emphasized that HL is a versatile ligand, which can induce both Ln and TM ions to undergo aggregation. This work not only expands the field of known high-nuclearity Ln clusters, but also is expected to promote progress in making high dimensional frameworks and highly connected nets.

ASSOCIATED CONTENT

Supporting Information

X-ray crystallographic file in CIF format for **1**−**2**, Tables S1 and S2, and additional figures of the coordination environments of the metal ions and IR, PXRD, TGA, and UV−vis details. This material is available free of charge via the Internet at http://pubs.acs.org.

AUTHOR INFORMATION

Corresponding Author

*E-mail: ygy@fjirsm.ac.cn.

Notes

The authors declare no competing financial interest.

ACKNOWLEDGMENTS

This work was supported by the NSFC (91122028, 21221001, and 50872133), the 973 Program (2014CB932101 and 2011CB932504), and the NSFC for Distinguished Young Scholars (20725101).

REFERENCES

(1) (a) Bai, J. F.; Virovets, A. V.; Scheer, M. *Science* **2003**, *300*, 781−783. (b) Lombardi, J. R.; Davis, B. *Chem. Rev.* **2002**, *102*, 2431−2460. (c) Huang, Y. G.; Jiang, F. L.; Hong, M. C. *Coord. Chem. Rev.* **2009**, *253*, 2814−2834.

(2) (a) Müller, A.; Beckmann, E.; Bögge, H.; Schmidtmann, M.; Dress, A. *Nature* **2002**, *41*, 1162−1167. (b) Tasiopoulos, A. J.; Vinslava, A.; Wernsdorfer, W.; Abboud, K. A.; Christou, G. *Angew. Chem., Int. Ed.* **2004**, *43*, 2117−2121.

(3) (a) Zhang, M. B.; Zhang, J.; Zheng, S. T.; Yang, G. Y. *Angew. Chem., Int. Ed.* **2005**, *44*, 1385−1388. (b) Zheng, S. T.; Wu, T.; Chou, C.; Fuhr, A.; Feng, P.; Bu, X. *J. Am. Chem. Soc.* **2012**, *134*, 4517−4520.

(4) (a) Hewitt, I. J.; Tang, J.; Madhu, N. T.; Anson, C. E.; Lan, Y.; Luzon, J.; Etienne, M.; Sessoli, R.; Powell, A. K. *Angew. Chem., Int. Ed.* **2010**, *49*, 6352−6356. (b) Yang, X. P.; Jones, R. A.; Wiester, M. J. *Dalton Trans.* **2004**, 1787−1788. (c) Wang, R. Y.; Selby, H. D.; Liu, H.; Carducci, M. D.; Jin, T. Z.; Zheng, Z. P.; Anthis, J. W.; Staples, R. J. *Inorg. Chem.* **2002**, *41*, 278−286. (d) Bürgstein, M. R.; Roesky, P. W. *Angew. Chem., Int. Ed.* **2000**, *39*, 549−551. (e) Kong, X. J.; Wu, Y. L.; Long, L. S.; Zheng, L. S.; Zheng, Z. P. *J. Am. Chem. Soc.* **2009**, *131*, 6918−6819.

(5) (a) Leng, J. D.; Liu, J. L.; Tong, M. L. *Chem. Commun.* **2012**, *48*, 5286−5288. (b) Xiang, S. C.; Hu, S. M.; Sheng, T. L.; Fu, R. B.; Wu, X. T.; Zhang, X. D. *J. Am. Chem. Soc.* **2007**, *129*, 15144−15146. (c) Zheng, Y. Z.; Evangelisti, M.; Winpenny, R. E. P. *Chem. Sci.* **2011**, *2*, 99−102.

(6) (a) Cheng, J. W.; Zhang, J.; Zheng, S. T.; Yang, G. Y. *Chem.—Eur. J.* **2008**, *14*, 88−97. (b) Fang, W. H.; Cheng, J. W.; Yang, G. Y. *Chem.—Eur. J.* **2014**, *20*, 2704−2711.

(7) Chen, X. M.; Aubin, S. M. J.; Wu, Y. L.; Yang, Y. S.; Mak, T. C. W.; Hendrickson, D. N. *J. Am. Chem. Soc.* **1995**, *117*, 9600−9601.

(8) (a) Cheng, J. W.; Zhang, J.; Zheng, S. T.; Zhang, M. B.; Yang, G. Y. *Angew. Chem., Int. Ed.* **2006**, *45*, 73−77. (b) Zhao, B.; Gao, H. L.; Chen, X. Y.; Cheng, P.; Shi, W.; Liao, D. Z.; Yan, S. P.; Jiang, Z. H. *Chem.—Eur. J.* **2005**, *12*, 149−158.

(9) (a) Zhang, Y. B.; Zhou, H. L.; Lin, R. B.; Zhang, C.; Lin, J. B.; Zhang, J. P.; Chen, X. M. *Nat. Commun.* **2012**, *3*, 642. (b) Yin, Z.; Wang, Q. X.; Zeng, M. H. *J. Am. Chem. Soc.* **2012**, *134*, 4857−4863. (c) Wang, Z. L.; Fang, W. H.; Yang, G. Y. *Chem. Commun.* **2010**, *46*, 8216−8218. (d) Fang, W. H.; Cheng, L.; Huang, L.; Yang, G. Y. *Inorg. Chem.* **2013**, *52*, 6−8. (e) Fang, W. H.; Yang, G. Y. *CrystEngComm* **2013**, *15*, 9504−9512.

(10) Poncelet, O.; Hubert-Pfalzgraf, L. G.; Daran, J. C.; Astierc, R. *Chem. Commun.* **1989**, 1846−1848.

(11) (a) Ke, H.; Xu, G. F.; Zhao, L.; Tang, J.; Zhang, X. Y.; Zhang, H. J. *Chem.—Eur. J.* **2009**, *15*, 10335−10338. (b) Ke, H.; Zhao, L.; Xu, G. F.; Guo, Y. N.; Tang, J.; Zhang, X. Y.; Zhang, H. J. *Dalton Trans.* **2009**, 10609−10613.

(12) Li, X.; Huang, Y.; Cao, R. *CrystEngComm* **2012**, *14*, 6045−6048.

(13) (a) Sheldrick, G. M. *SHELXS97, Program for Crystal Structure Solution*; University of Göttingen: Göttingen, Germany, 1997. (b) Sheldrick, G. M. *SHELXL97, Program for Crystal Structure Refinement*; University of Göttingen: Göttingen, Germany, 1997.

(14) Plečnik, C. E.; Liu, S.; Shore, S. G. *Acc. Chem. Res.* **2003**, *36*, 499−508.

(15) (a) Rizzi, A. C.; Calvo, R.; Baggio, R.; Garland, M. T.; Pena, O.; Perec, M. *Inorg. Chem.* **2001**, *41*, 5609−5614. (b) Liu, Q. D.; Li, J. R.; Gao, S.; Ma, B. Q.; Liao, F. H.; Zhou, Q. Z.; Yu, K. B. *Inorg. Chem. Commun.* **2001**, *4*, 301−304.
(16) (a) Yao, Y. L.; Che, Y. X.; Zheng, J. M. *Cryst. Growth Des.* **2008**, *8*, 2299−2306. (b) Wang, Z. X.; Wu, Q. F.; Liu, H. J.; Shao, M.; Xiao, H. P.; Li, M. X. *CrystEngComm* **2010**, *12*, 1139−1146.
(17) Calvez, G.; Daiguebonne, C.; Guillou, O. *Inorg. Chem.* **2011**, *50*, 2851−2858.
(18) Zheng, S. T.; Yuan, D. Q.; Jia, H. P.; Zhang, J.; Yang, G. Y. *Chem. Commun.* **2007**, 1858−1860.
(19) Zhang, H. X.; Zhang, J.; Zheng, S. T.; Yang, G. Y. *Inorg. Chem.* **2003**, *42*, 6595−6597.
(20) Cheng, J. W.; Zheng, S. T.; Yang, G. Y. *Inorg. Chem.* **2008**, *47*, 4930−4935.
(21) (a) Peng, R.; Li, M.; Li, D. *Coord. Chem. Rev.* **2010**, *254*, 1−18. (b) Hartl, H.; Fuchs, J. *Angew. Chem., Int. Ed. Engl.* **1986**, *25*, 569−570. (c) Sarkar, M.; Biradha, K. *Chem. Commun.* **2005**, 2229−2231.
(22) (a) Cheng, L.; Wei, Q.; Wu, H. Q.; Zhou, L. J.; Yang, G. Y. *Chem.—Eur. J.* **2013**, *19*, 17662−17667. (b) Wang, M. S.; Guo, G. C.; Chen, W. T.; Xu, G.; Zhou, W. W.; Wu, K. J.; Huang, J. S. *Angew. Chem., Int. Ed.* **2007**, *46*, 3909−3911.
(23) Huang, L.; Cheng, L.; Fang, W. H.; Wang, S. S.; Yang, G. Y. *Eur. J. Inorg. Chem.* **2013**, 1693−1698.
(24) (a) Lin, Z. J.; Liu, T. F.; Xu, B.; Han, L. W.; Huang, Y. B.; Cao, R. *CrystEngComm* **2011**, *13*, 3321−3324. (b) Lin, Z. E.; Zhang, J.; Zheng, S. T.; Yang, G. Y. *Microporous Mesoporous Mater.* **2004**, *68*, 65−70.
(25) Xia, J.; Zhao, B.; Wang, H. S.; Shi, W.; Ma, Y.; Song, H. B.; Cheng, P.; Liao, D. Z.; Yan, S. P. *Inorg. Chem.* **2007**, *46*, 3450−3458.
(26) (a) Bo, Q. B.; Sun, G. X.; Geng, D. L. *Inorg. Chem.* **2009**, *49*, 561−571. (b) Cai, S. L.; Zheng, S. R.; Wen, Z. Z.; Fan, J.; Zhang, W. G. *Cryst. Growth Des.* **2012**, *12*, 5737−5745.
(27) (a) Li, X. F.; Huang, Y. B.; Cao, R. *Cryst. Growth Des.* **2012**, *12*, 3549−3556. (b) Gu, X. J.; Xue, D. F. *Inorg. Chem.* **2007**, *46*, 5349−5353.
(28) Blatov, V. A.; Shevchenko, A. P.; Serezhkin, V. N. *J. Appl. Crystallogr.* **2000**, *33*, 1193.
(29) (a) Zhang, X. M.; Fang, R. Q.; Wu, H. S. *J. Am. Chem. Soc.* **2005**, *127*, 7670−7671. (b) Hao, Z. M.; Fang, R. Q.; Wu, H. S.; Zhang, X. M. *Inorg. Chem.* **2008**, *47*, 8197.
(30) Hill, R. J.; Long, D. L.; Champness, N.; Hubberstey, P.; Schröder, M. *Acc. Chem. Res.* **2005**, *38*, 337−350.
(31) (a) Kubelka, P.; Munk, F. *Z. Technol. Phys.* **1931**, *12*, 593−601. (b) Wendlandt, W. W.; Hecht, H. G. *Reflectance Spectroscopy*; Wiley-Interscience: New York, 1966.

dx.doi.org/10.1021/ic500404z | *Inorg. Chem.* 2014, 53, 5631−5636